Mobility edges in bichromatic optical lattices

Dave J. Boers, Benjamin Goedeke, Dennis Hinrichs, and Martin Holthaus*
Institut für Physik, Carl von Ossietzky Universität, D-26111 Oldenburg, Germany
(Received 21 January 2007; published 6 June 2007)

We investigate the localization properties of single-particle eigenstates in bichromatic one-dimensional optical lattices. Whereas such a lattice with a sufficiently deep primary component and a suitably adjusted incommensurate secondary component provides an approximate realization of the Harper model, the system's self-duality is broken when the lattice is comparatively shallow. As a consequence, the sharp metal-insulator transition exhibited by Harper's model is replaced by a sequence of mobility edges in realistic bichromatic optical lattices that do not reach the tight-binding regime.

DOI: 10.1103/PhysRevA.75.063404 PACS number(s): 32.80.Lg, 71.23.An, 72.15.Rn, 03.65.−w

I. INTRODUCTION

The deceptively simple single-band tight-binding model given by the Hamiltonian $H_{\mathrm{tb}}=H_{\mathrm{nn}}+H_{\mathrm{os}}$, where

$$H_{\mathrm{nn}}=\sum_{\ell=-\infty}^{+\infty}\frac{t}{2}(|\ell\rangle\langle\ell+1|+|\ell+1\rangle\langle\ell|) \tag{1}$$

describes a single particle moving on a one-dimensional lattice with constant hopping matrix elements $t/2$ connecting each Wannier state $|\ell\rangle$ with its two nearest neighbors, and

$$H_{\mathrm{os}}=\sum_{\ell=-\infty}^{+\infty}v\cos(2\pi g\ell+\delta)|\ell\rangle\langle\ell| \tag{2}$$

introduces a modulation of the on-site energies with amplitude v, possesses unusual properties [1]. Provided the number g is irrational, and $|v/t|<1$, all its energy eigenstates are extended, but they become exponentially localized when $|v/t|>1$, with a sharp metal-insulator transition occurring at $|v/t|=1$ [1,2]. At the transition point, the energy spectrum is fractal: If one plots the eigenvalues for $|v/t|=1$ versus g, one obtains the famous Hofstadter butterfly [3,4]. Accordingly, this system has attracted a lot of interest [5–8].

A possible experimental realization could exploit ultracold atoms of mass m in a superposition of two standing laser light waves directed along the x axis with wave numbers k_L and gk_L. Atomic motion along the lattice is then described by the effective Hamiltonian $H=H_0+H_1$, where

$$H_0=\frac{p^2}{2m}-\frac{V_0}{2}\cos(2k_Lx) \tag{3}$$

models a monochromatic optical lattice with period $d=\pi/k_L$, and

$$H_1=V_1\cos(2gk_Lx+\delta) \tag{4}$$

describes a second cosine lattice which, for irrational g, is incommensurate with the first one, δ being an arbitrary phase. If the depth V_0 of the "principal" component of such a bichromatic optical lattice is chosen sufficiently large compared to the recoil energy $E_r=\hbar^2k_L^2/(2m)$, such that the single-particle dynamics can be restricted to the lowest Bloch band given by H_0, and the corresponding lowest-band Wannier states have appreciable overlap with their nearest neighbors only, the monochromatic lattice (with $V_1/E_r=0$) provides a good approximation to the basic tight-binding model H_{nn} [9]. If then the second optical lattice component modeled by H_1 is added, with an amplitude V_1 that is merely on the order of the width of the lowest Bloch band of the primary lattice, one obtains an approximation to the full system H_{tb} [10,11]. In view of the enormous experience that has been gained recently with ultracold atoms in periodic optical lattices [12,13], culminating in the observation of the transition from a superfluid to a Mott insulator [14,15], and in the realization of the Tonks-Girardeau gas [16], it seems promising now to start exploring quasiperiodic optical lattice structures [17].

The metal-insulator transition exhibited by the tight-binding model $H_{\mathrm{tb}}=H_{\mathrm{nn}}+H_{\mathrm{os}}$ hinges on a delicate property. If one expands its energy eigenfunctions in the form

$$|\psi_E\rangle=\sum_{\ell=-\infty}^{\infty}a_\ell|\ell\rangle, \tag{5}$$

the stationary Schrödinger equation translates into

$$\frac{t}{2}(a_{\ell+1}+a_{\ell-1})+v\cos(2\pi g\ell+\delta)a_\ell=Ea_\ell, \tag{6}$$

a system known as the Aubry-André model [1], or as Harper's equation [8]. Considering then the transformation

$$a_\ell=\sum_m b_m e^{im(2\pi g\ell+\delta)}e^{i\beta\ell}, \tag{7}$$

which maps the set of amplitudes $\{a_\ell\}$ to its dual $\{b_m\}$, this equation (6) is cast into the form

$$\frac{v}{2}(b_{m+1}+b_{m-1})+t\cos(2\pi gm+\beta)b_m=Eb_m, \tag{8}$$

with the same eigenvalue E. Thus, the system (6) possesses self-duality: Its dual equation (8) has precisely the same form, with the roles of t and v being interchanged [2].

It is immediately obvious that this self-duality can be "broken" in a realistic one-dimensional lattice which, unlike the theoretical ideal described by H_{tb}, does admit not only

*Electronic address: holthaus@theorie.physik.uni-oldenburg.de

 ©2007 The American Physical Society

coupling between neighboring Wannier states, but also next-to-nearest neighbor interactions, and possibly interactions between Wannier states separated still farther from each other. This happens in a bichromatic optical lattice of the type sketched above, when the primary lattice which defines the Wannier basis does not reach the tight-binding limit. It is, therefore, both of interest and of relevance to investigate how the sharp transition featured by H_{tb} is affected in an imperfect realization achieved with moderately deep optical lattices, when self-duality is not ensured.

Thus, in this paper we consider the dynamics of a single particle in a bichromatic optical lattice beyond the tight-binding limit. In the following section we study the exact Wannier states for monochromatic cosine lattices, and quantify the magnitude of next-to-nearest-neighbor coupling. In Sec. III, we then demonstrate that the sharp metal-insulator transition met in the ideal tight-binding model H_{tb} gives way to a sequence of mobility edges in comparatively shallow bichromatic optical lattices, and briefly draw some conclusions in Sec. IV.

II. WANNIER FUNCTIONS FOR A COSINE LATTICE

Our deductions are based on an inspection of the Wannier functions [18] pertaining to the lowest energy band of the primary cosine lattice (3) with depth V_0. Wannier functions do depend on the choice of the phases of the Bloch waves from which they are computed; we consider here the maximally localized, real Wannier functions as specified by Kohn [19]. It is intuitively clear that within a sufficiently deep cosine well a Wannier function $w_0(x)$ is approximated by the harmonic-oscillator ground state function adapted to the well's parabolic bottom [20]

$$\phi_0(x) = \frac{k_L^{1/2}}{\pi^{1/4}}\left(\frac{V_0}{E_r}\right)^{1/8} \exp\left(-\frac{1}{2}\sqrt{\frac{V_0}{E_r}}(k_L x)^2\right). \tag{9}$$

However, there are profound differences between this Gaussian and the true Wannier functions: On the one hand, the tails of the actual Wannier functions oscillate, in order to ensure orthogonality of functions centered at different lattice sites. On the other hand, the asymptotic decay of the exact functions is given (for $x>0$) by

$$w_0(x) \sim x^{-3/4} \exp(-h_0 x), \tag{10}$$

where h_0 is the (positive) imaginary part of the branch point connecting the lowest two energy bands in the complex k plane [19], and the universal exponent $-3/4$ of the prefactor is due to the fact that this branch point is of the square-root type [21]. In Fig. 1 we compare the local Gaussian (9) to the exact Wannier function for a monochromatic cosine lattice with depth $V_0/E_r=3$, while Fig. 2 visualizes the exponential decay of the exact function.

Now the nth Fourier component of the dispersion $E(k)$ for the lowest energy band

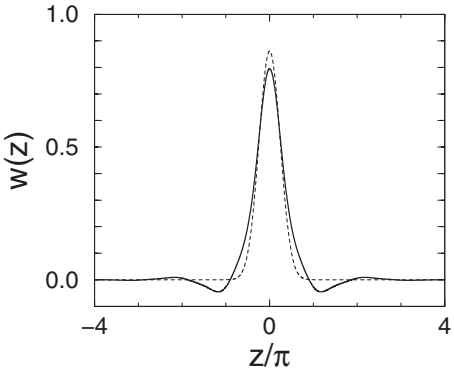

FIG. 1. Wannier function $w_0(z)$ for the lowest energy band of a monochromatic cosine lattice (3) with depth $V_0/E_r=3$ (full line), compared to its harmonic-oscillator approximation (9) (dashes). We employ the dimensionless coordinate $z=k_L x$, so that $\Delta z=\pi$ corresponds to one lattice period.

$$E(k) = E_0 + \sum_{n=1}^{\infty} (-1)^n 2J_n \cos(nkd) \tag{11}$$

is given by the matrix element of the monochromatic lattice Hamiltonian (3) taken with Wannier functions $w_0(x)$ and $w_n(x)=w_0(x-nd)$ located at sites separated by n lattice periods d,

$$(-1)^n J_n = \langle w_0|H_0|w_n\rangle. \tag{12}$$

Hence, under conditions such that it suffices to retain only $n=\pm 1$, i.e., only nearest-neighbor interaction, the Wannier representation of H_0 reduces to the model (1) with $t/2=-J_1$, neglecting the overall energy shift E_0. However, in many cases this reduction is an oversimplification. According to He and Vanderbilt [21], the decay of the matrix elements (12) with n is again described by an asymptotic law of the type (10),

$$J_n \sim (nd)^{-3/2} \exp(-h_0 nd), \tag{13}$$

with modified universal exponent $-3/2$ of the prefactor. Hence, knowledge of the branch point h_0 is of key importance for estimating the magnitude of the interaction among non-neighboring Wannier states. A weak-binding calculation yields

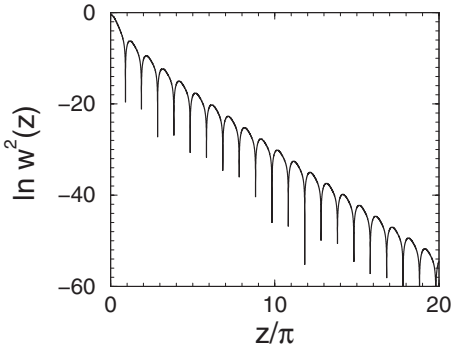

FIG. 2. Decay of the square of the exact Wannier function $w_0(z)$ depicted in Fig. 1.

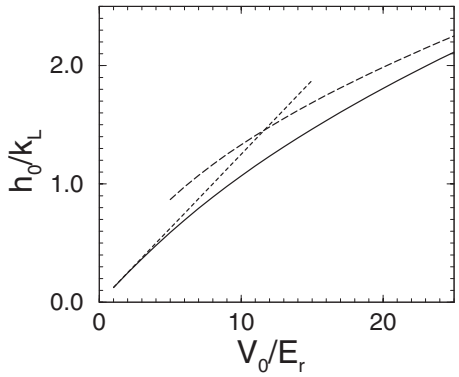

FIG. 3. Location of the branch point h_0/k_L, as a function of the depth V_0/E_r of a monochromatic cosine lattice (full line). Also shown are the estimates (14) (short dashes) and (15) (long dashes).

$$h_0/k_L \approx \frac{V_0}{8E_r} \quad \text{for} \quad \frac{V_0}{4E_r} \ll 1, \tag{14}$$

whereas an estimate based on the known properties of the Mathieu equation [22] leads to the relation

$$h_0/k_L \sim \sqrt{\frac{V_0}{4E_r}} - \frac{1}{4} \tag{15}$$

for very deep lattices. Figure 3 shows numerically computed, exact values of h_0/k_L; the two trends (14) and (15) are clearly recognizable.

In order to assess the accuracy of the asymptotic law (13), we plot in Fig. 4 the quantities $\ln(J_n/E_r)+n\pi h_0/k_L$ versus $\ln n\pi$ for $V_0/E_r=3$. According to Eq. (13), one expects a straight line with slope $-3/2$ for large n; actually, this expectation is well met even for small n.

To conclude the investigation of the Wannier basis for the monochromatic cosine lattice (3), we list some typical numerical data in Table I. The large squared overlap $|\langle w_0|\phi_0\rangle|^2$ of the Gaussian (9) with the true Wannier function already for low V_0/E_r should not divert attention from the essential point: For $V_0/E_r=3$ the ratio J_2/J_1 of the magnitude of next-to-nearest-neighbor coupling J_2 to nearest-neighbor coupling J_1 is still on the order of 10%. This ratio drops to 1% when $V_0/E_r=10$, and becomes 0.1% when $V_0/E_r=20$. In other words, the description of optical lattice potentials in terms of a nearest-neighbor model becomes correct at the one-percent level only when $V_0/E_r \gtrsim 10$.

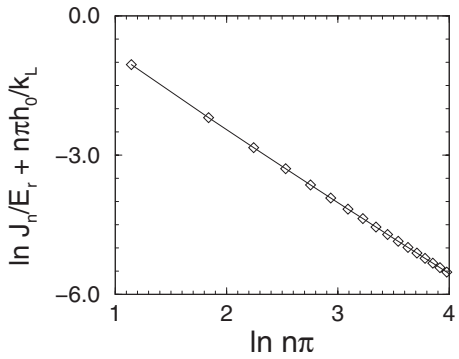

FIG. 4. Plot of $\ln(J_n/E_r)+n\pi h_0/k_L$ vs $\ln n\pi$ for $V_0/E_r=3$ (diamonds), using $h_0/k_L=0.3661$. The slope $-3/2$ expected for large n is already showing up for small n.

TABLE I. Numerical values characterizing optical cosine lattices for some typical depths V_0/E_r.

V_0/E_r	$\lvert\langle w_0\rvert\phi_0\rangle\rvert^2$	h_0/k_L	J_1/E_r	J_2/J_1
3.0	0.9719	0.3661	0.11103	0.1011
5.0	0.9836	0.5896	0.06577	0.0516
10.0	0.9938	1.0678	0.01918	0.0118
15.0	0.9964	1.4635	0.00652	0.0035
20.0	0.9975	1.8069	0.00249	0.0012
25.0	0.9981	2.1144	0.00104	0.0005

III. MOBILITY EDGES

We now turn to bichromatic optical lattices as given by Eqs. (3) and (4), with the understanding that the amplitude V_1 of their secondary component remains small compared to the depth V_0 of the principal one. In order to characterize the localization properties of the eigenstates of such a system, we diagonalize the full Hamiltonian $H=H_0+H_1$ in the lowest-band Wannier basis defined by the principal lattice H_0, after truncating that lattice to a finite number N of sites. From the expansion of the αth eigenstate

$$\psi_\alpha(x) = \sum_{\ell=1}^{N} a_\ell^\alpha w_\ell(x), \tag{16}$$

with $w_\ell(x)=w_0(x-\ell d)$, we then compute its extension σ_α,

$$\sigma_\alpha = \sqrt{\frac{12}{N^2-1}}\left[\sum_{\ell=1}^{N} \ell^2 |a_\ell^\alpha|^2 - \left(\sum_{\ell=1}^{N} \ell |a_\ell^\alpha|^2\right)^2\right]^{1/2}, \tag{17}$$

normalized such that $\sigma_\alpha=1$ for a uniformly extended state (i.e., when $a_\ell^\alpha=1/\sqrt{N}$ for all sites ℓ). Then

$$\bar{\sigma} = \frac{1}{N}\sum_{\alpha=1}^{N} \sigma_\alpha \tag{18}$$

provides a measure for the average extension of the eigenstates, with $\bar{\sigma}\approx 1$ implying that most eigenstates are extended all over the (truncated) lattice, whereas $\bar{\sigma}\approx 0$ indicates that all eigenstates are strongly localized. Figure 5 summarizes results of such calculations for various depths V_0 of the principal lattice, as functions of the perturbation V_1 introduced by the second component. In all these calculations we fix $g=(\sqrt{5}-1)/2$ as the incommensurability parameter, and choose $N=1000$. Evidently, $\bar{\sigma}$ drops sharply with increasing V_1/E_r from 1 to about 0 when the primary lattice is deep, $V_0/E_r \gtrsim 10$, thus indicating an approximate realization of the sharp metal-insulator transition predicted by the ideal tight-binding model H_{tb}. In contrast, $\bar{\sigma}$ features pronounced steps when the primary lattice is shallow, $V_0/E_r \lesssim 5$. These steps are a clear manifestation of the effect of the residual next-to-nearest- (and higher) neighbor cou-

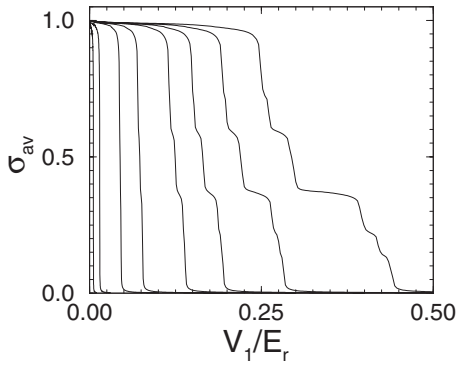

FIG. 5. Average extension $\sigma_{\mathrm{av}}=\bar{\sigma}$ for the eigenstates of bichromatic optical lattices, as functions of the amplitude V_1 of the secondary lattice (4), with incommensurability parameter $g=(\sqrt{5}-1)/2$. The amplitudes of the principal lattices (3) are $V_0/E_r=3,4,5,6,8,10,15,20$ (right to left).

plings quantified in Table I, and discarded in Harper's equation (6).

To throw light on the nature of these steps, we plot in Fig. 6 the extensions σ_α of the individual energy eigenstates versus their respective energy E, each dot corresponding to one state, for the most shallow primary lattice considered in Fig. 5, with $V_0/E_R=3.0$. In Fig. 6(a) we have $V_1/E_R=0.25$, coinciding roughly with the onset of the steep drop of the corresponding line in Fig. 5; $V_1/E_R=0.293$ in (b), located in the middle between the first two well-developed steps; and $V_1/E_R=0.35$ in (c), in the middle of the most pronounced plateau. In general, energy eigenvalues for an infinite quasiperiodic lattice form an intricate pattern of subbands and gaps [17,23], a glimpse of which can be inferred, even for only $N=1000$, from the pattern of the eigenvalues displayed in Fig. 6. We have made sure that the structure of these plots remains practically unchanged when the number of sites is increased to $N=2000$. Evidently, when V_1/E_r is increased, the eigenstates investigated here do not all localize simultaneously, as they do in the tight-binding model H_{tb}, but rather subband by subband, so that within an intermediate regime of V_1/E_r localized states in "lower" subbands coexist with extended states in "higher" ones, i.e., there are mobility edges. Thus, as a consequence of the "breaking" of Aubry-André self-duality occurring in shallow bichromatic optical lattices, resulting from (predominantly) next-to-nearest-neighbor interaction, the sharp metal-insulator transition shown by the ideal tight-binding model H_{tb} is replaced by a sequence of mobility edges.

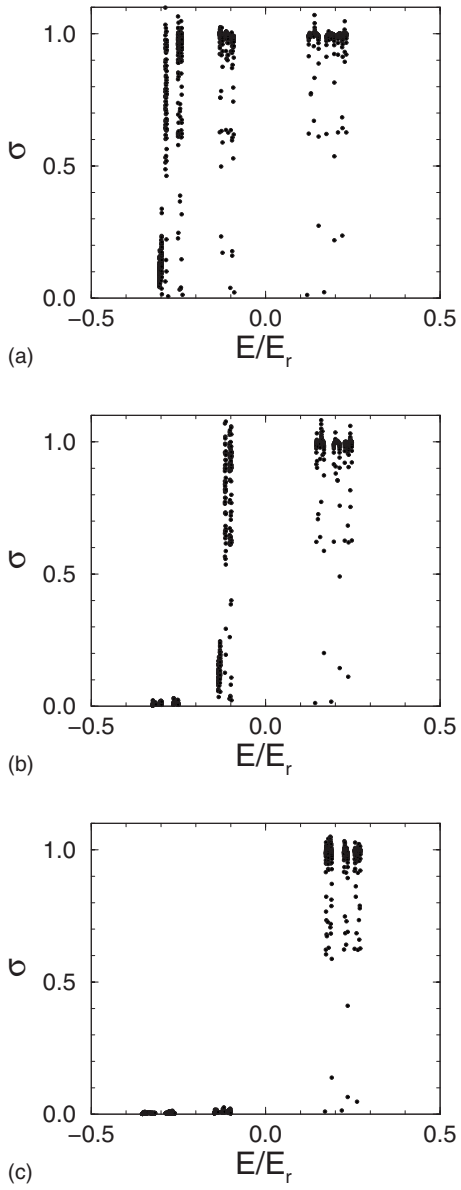

FIG. 6. Extensions σ_α of individual eigenstates of a bichromatic optical lattice, with depth $V_0/E_r=3$ of the primary component. As in Fig. 5, we set $g=(\sqrt{5}-1)/2$ and $N=1000$. The amplitudes of the secondary lattices are $V_1/E_r=0.25$ (a), 0.293 (b), and 0.35 (c).

IV. CONCLUSION

One-dimensional quasiperiodic lattice structures show features far more delicate than the usual Bloch bands encountered in periodic lattices, and fairly different from lattices with truly random disorder. Although the mathematical theory of such systems governed by almost periodic Schrödinger operators is quite well developed [23], their experimental study still rests in its infancy. Hall measurements on a two-dimensional electron gas in a semiconductor superlattice indeed have revealed traces of the Hofstadter butterfly spectrum [24]. But still, there exists a need for more versatile and well controllable laboratory realizations of quasiperiodic systems.

With the ubiquitous availability of cold atoms in optical lattices [12,13], and the possibility to realize bichromatic optical lattices, this situation is likely to change in the near future. In particular, we have suggested in this paper to consider one-dimensional bichromatic lattices with a sufficiently strong primary component (3), and a secondary component with an amplitude that is comparable to the width of the lowest Bloch band defined by the primary lattice. As witnessed by Fig. 5, such a system provides an approximate realization of the sharp metal-insulator transition exhibited by the ideal Harper model (6) when the primary lattice is at

least ten recoil energies deep, so that only the coupling between Wannier states adjacent to each other remains appreciable. In a laboratory experiment, such a transition could be detected by measuring the momentum distribution of the atoms, or by studying the diffusion of their wave packets [17]. Our model calculations show that it is not necessary to implement truly irrational numbers with mathematical (i.e., unattainable) precision; after all, on a finite lattice one can "resolve" only a finite number of digits.

From the condition $|v/t|=1$ for the transition in the model (6), one can derive an estimate for the "critical" amplitude V_1^c of the secondary lattice, given the depth V_0 of the primary one: When $V_0/E_r \gtrsim 10$, the hopping matrix element $-t/2$ appearing in Eq. (1) is well approximated by [25]

$$-\frac{t}{2} \sim \frac{4E_r}{\sqrt{\pi}}\left(\frac{V_0}{E_r}\right)^{3/4} \exp\left(-2\sqrt{\frac{V_0}{E_r}}\right). \tag{19}$$

On the other hand, the amplitude v of the on-site perturbation (2) can be estimated with the help of the Gaussian approximation (9) for the Wannier states as follows:

$$v \sim \langle \phi_0 | H_1 | \phi_0 \rangle = V_1 \exp\left(-\frac{g^2}{\sqrt{V_0/E_r}}\right). \tag{20}$$

This gives

$$\frac{V_1^c}{E_r} \sim \frac{8}{\sqrt{\pi}}\left(\frac{V_0}{E_r}\right)^{3/4} \exp\left(+\frac{g^2}{\sqrt{V_0/E_r}} - 2\sqrt{\frac{V_0}{E_r}}\right), \tag{21}$$

valid for reasonably chosen g on the order of unity.

Perhaps even more interesting than an approximate realization of Harper's model (6) with deep primary lattices is the appearance of mobility edges, and the associated coexistence of extended and localized single-particle eigenstates, in comparatively shallow bichromatic lattices. Actually, the estimate (21) does not only yield the "critical" modulation strength V_1^c when the primary lattice is deep, but it also gives a reasonable idea of the amplitudes V_1 required for inducing such mobility edges in more shallow lattices. In Fig. 7 we compare the estimate (21) with those values of V_1 which, according to Fig. 5, lead to an average extension of $\bar{\sigma}=0.5$. Evidently, the agreement is satisfactory even beyond the tight-binding limit.

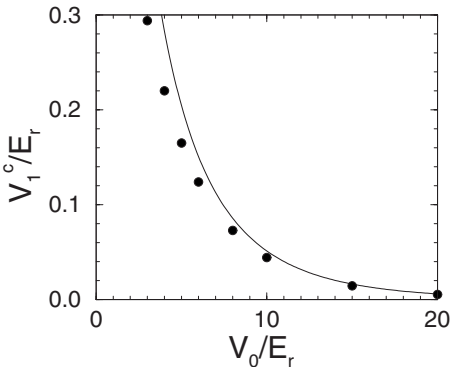

FIG. 7. Comparison of the estimate (21) for $g=(\sqrt{5}-1)/2$ (full line) with those values of V_1/E_r which lead to an average extension of $\bar{\sigma}=0.5$ (dots), as determined from Fig. 5.

We suggest that possible laboratory experiments with bichromatic lattices aiming for the detection of these mobility edges should employ primary components with a depth of three recoil energies or even less, which are readily available [12–14]. According to Fig. 5, detection of the main edges then requires adjusting the depth of the secondary component with a precision of about $0.05E_r$.

With a view towards promising future developments, it would be interesting to consider not only single-particle phenomena, but also to investigate Bose-Einstein condensates in bichromatic optical lattices of the type suggested here. In that case, the incommensurability-induced transition described by the ideal Harper model would compete with the interaction-induced Mott-Hubbard transition [14,15], and it might be worthwhile to study the outcome of that competition.

ACKNOWLEDGMENTS

This work was supported in part by the Deutsche Forschungsgemeinschaft through the Priority Programme SPP 1116. M.H. also thanks W. Zwerger for an insightful discussion on Wannier functions.

[1] J. B. Sokoloff, Phys. Rep. **126**, 189 (1985).
[2] S. Aubry and G. André, Ann. Isr. Phys. Soc. **3**, 133 (1980).
[3] D. R. Hofstadter, Phys. Rev. B **14**, 2239 (1976).
[4] D. Jaksch and P. Zoller, New J. Phys. **5**, 56 (2003).
[5] D. J. Thouless, Phys. Rev. B **28**, 4272 (1983).
[6] D. J. Thouless, Commun. Math. Phys. **127**, 187 (1990).
[7] A. Rüdinger and F. Piéchon, J. Phys. A **30**, 117 (1997).
[8] S. N. Evangelou and J.-L. Pichard, Phys. Rev. Lett. **84**, 1643 (2000).
[9] D. Jaksch and P. Zoller, Ann. Phys. (N.Y.) **315**, 52 (2005).
[10] K. Drese and M. Holthaus, Phys. Rev. Lett. **78**, 2932 (1997).
[11] K. Drese and M. Holthaus, Chem. Phys. **217**, 201 (1997).
[12] M. Weitz, G. Cennini, G. Ritt, and C. Geckeler, Phys. Rev. A **70**, 043414 (2004).
[13] O. Morsch and M. K. Oberthaler, Rev. Mod. Phys. **78**, 179 (2006).
[14] M. Greiner, O. Mandel, T. Esslinger, T. W. Hänsch, and I. Bloch, Nature (London) **415**, 39 (2002).
[15] T. Stöferle, H. Moritz, C. Schori, M. Köhl, and T. Esslinger, Phys. Rev. Lett. **92**, 130403 (2004).
[16] B. Paredes, A. Widera, V. Murg, O. Mandel, S. Fölling, I. Cirac, G. V. Shlyapnikov, T. W. Hänsch, and I. Bloch, Nature (London) **429**, 277 (2004).
[17] R. B. Diener, G. A. Georgakis, J. Zhong, M. Raizen, and Q. Niu, Phys. Rev. A **64**, 033416 (2001).
[18] G. H. Wannier, Phys. Rev. **52**, 191 (1937).

[19] W. Kohn, Phys. Rev. **115**, 809 (1959).
[20] J. C. Slater, Phys. Rev. **87**, 807 (1952).
[21] L. He and D. Vanderbilt, Phys. Rev. Lett. **86**, 5341 (2001).
[22] *Handbook of Mathematical Functions*, edited by M. Abramowitz and I. A. Stegun (Dover, New York, 1972).
[23] B. Simon, Adv. Appl. Math. **3**, 463 (1982).
[24] C. Albrecht, J. H. Smet, K. von Klitzing, D. Weiss, V. Umansky, and H. Schweizer, Phys. Rev. Lett. **86**, 147 (2001).
[25] W. Zwerger, J. Opt. B: Quantum Semiclassical Opt. **5**, S9 (2003).